AER/AGS Open File Report 2020-02

Alberta Energy Regulator

Mapping Formation-Top Offsets in the Southwestern Alberta Plains, Canada: Methodology and Results

AGS 100 YEARS
ALBERTA GEOLOGICAL SURVEY

AER/AGS Open File Report 2020-02

Mapping Formation-Top Offsets in the Southwestern Alberta Plains, Canada: Methodology and Results

S. Mei and R. Schultz

Alberta Energy Regulator
Alberta Geological Survey

October 2020

ISBN 978-1-4601-4606-07

Mei, S and R. Schultz (2020): Mapping formation-top offsets in the southwestern Alberta Plains, Canada: methodology and results; Alberta Energy Regulator / Alberta Geological Survey, AER/AGS Open File Report 2020-02, 34 p.

Published October 2020 by:
Alberta Energy Regulator
Alberta Geological Survey
4th Floor, Twin Atria Building
4999 – 98th Avenue
Edmonton, AB T6B 2X3
Canada

Tel: 780.638.4491
Fax: 780.422.1459
Email: AGS-Info@aer.ca
Website: www.ags.aer.ca

Contents

Tables

Figures

Acknowledgements

We wish to thank D.I. Pană, D. Palombi, K.E. MacCormack, T.E. Hauck, M. Grobe, and K. Haug, whose editorial review and technical commentaries considerably improved the manuscript.

Abstract

This report presents the results of subsurface bedrock structure mapping in southwestern Alberta, Canada, using a methodology that assesses formation-top offsets. Three stratigraphic horizons were selected for mapping subsurface bedrock offsets: the base of the Fish Scales Formation, the top of the Milk River Formation, and the lower Bearpaw Formation flooding surface. The selected surfaces represent, or are close to, marine flooding surfaces in this area and can be considered to approximate a flat-lying surface (datum) and, therefore, are ideal for mapping post-depositional structures. A bedrock offset is defined in this report as any lineament or possible vertical displacement of a bedrock horizon that has been detected using geostatistical analysis of well-log data. This methodology identified numerous potential offsets which have been highlighted using residual maps of these three surfaces. The offset features identified from these surfaces were compared to each other, and to an isopach map of the interval from the base of the Fish Scales Formation to the top of Milk River Formation to evaluate whether these offsets represent potential growth faults. Some of the offsets mapped in this report were found to coincide with previously reported faults, which were identified at isolated riverbank outcrops and interpreted from seismic reflection surveys, and allow for determination of fault orientation and extent. The other offsets highlighted in this report may represent potential faults or differential compaction and highlight areas of geological interest for future structural analysis.

1 Introduction

In recent years, the Exshaw Formation and adjacent units, the underlying carbonates of the Big Valley and upper Stettler formations and the overlying basal Banff Formation, have emerged as unconventional tight oil resource plays in southwestern Alberta with the advent of hydraulic fracturing (fracking) techniques in horizontal wells. As a result, this area has experienced increased oil and gas development activities and capital investment since 2009 (Zaitlin et al., 2011). The AGS seismicity monitoring network detected a cluster of earthquakes in southwestern Alberta, which may be related to fault reactivation potentially induced by hydraulic fracturing (Schultz et al., 2015). Further investigation into this cluster of earthquakes requires detailed study of the bedrock structure, which may have significant impact on induced seismic events in this area.

This study attempts to map subsurface formation-top offsets in southwestern Alberta using well-log data and geostatistical analysis. We define an offset as any lineament of relatively abrupt elevation change of a formation top or bedrock horizon that can be detected using the methodology proposed by Mei (2009). This methodology enhances the identification of potential structures such as faults with offsets that are beyond the resolution of conventional stratigraphic contouring, seismic reflection profiles, and well-log cross-section methods.

A bedrock offset is defined in this report as any vertical displacement of a formation top or bedrock horizon, which may represent a potential fault in the study area; in other areas (e.g., west-central Alberta), a bedrock offset could also represent differential compaction over reefs and paleochannels (Mei, 2020). The study area extends from Twp. 1 (southern order with the U.S.) to Twp. 18 and from Rge. 13, W 4th Mer., to Rge. 2, W 5th Mer. The southwestern boundary of the study area corresponds to the approximate eastern limit of the deformation front of the Rocky Mountain fold-and-thrust belt (Figure 1). The base of the Fish Scales Formation (BFS), the top of the Milk River Formation, and the lower Bearpaw Formation flooding surface were selected for mapping subsurface bedrock offsets (Figure 2). Numerous linear offset structures were identified in these three surfaces. Some of the mapped offsets coincide with previously reported faults in various studies; one of the mapped offsets has been confirmed to be a fault by a later study (Galloway et al., 2018).

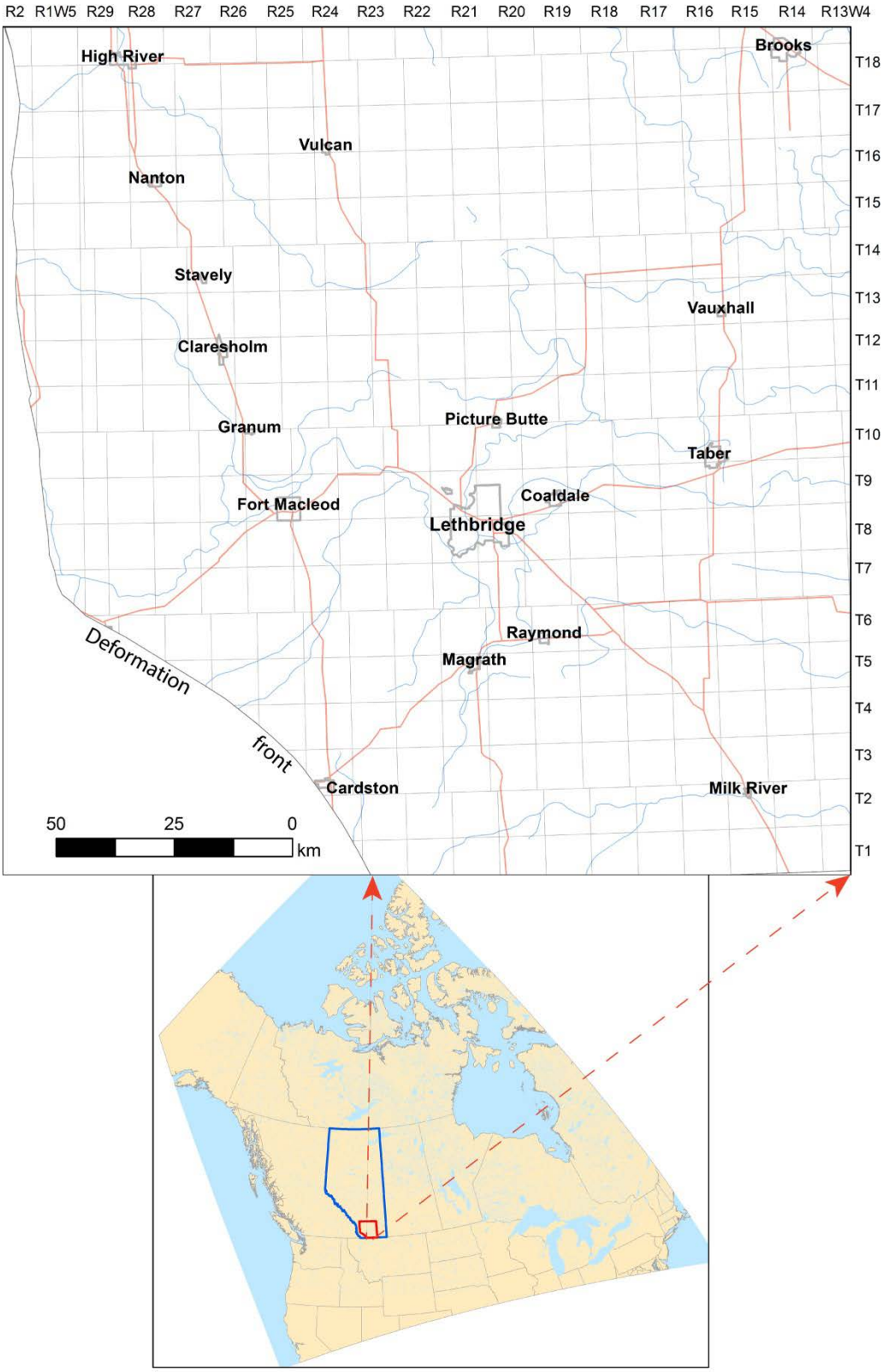

Figure 1. Location of the study area in southwestern Alberta.

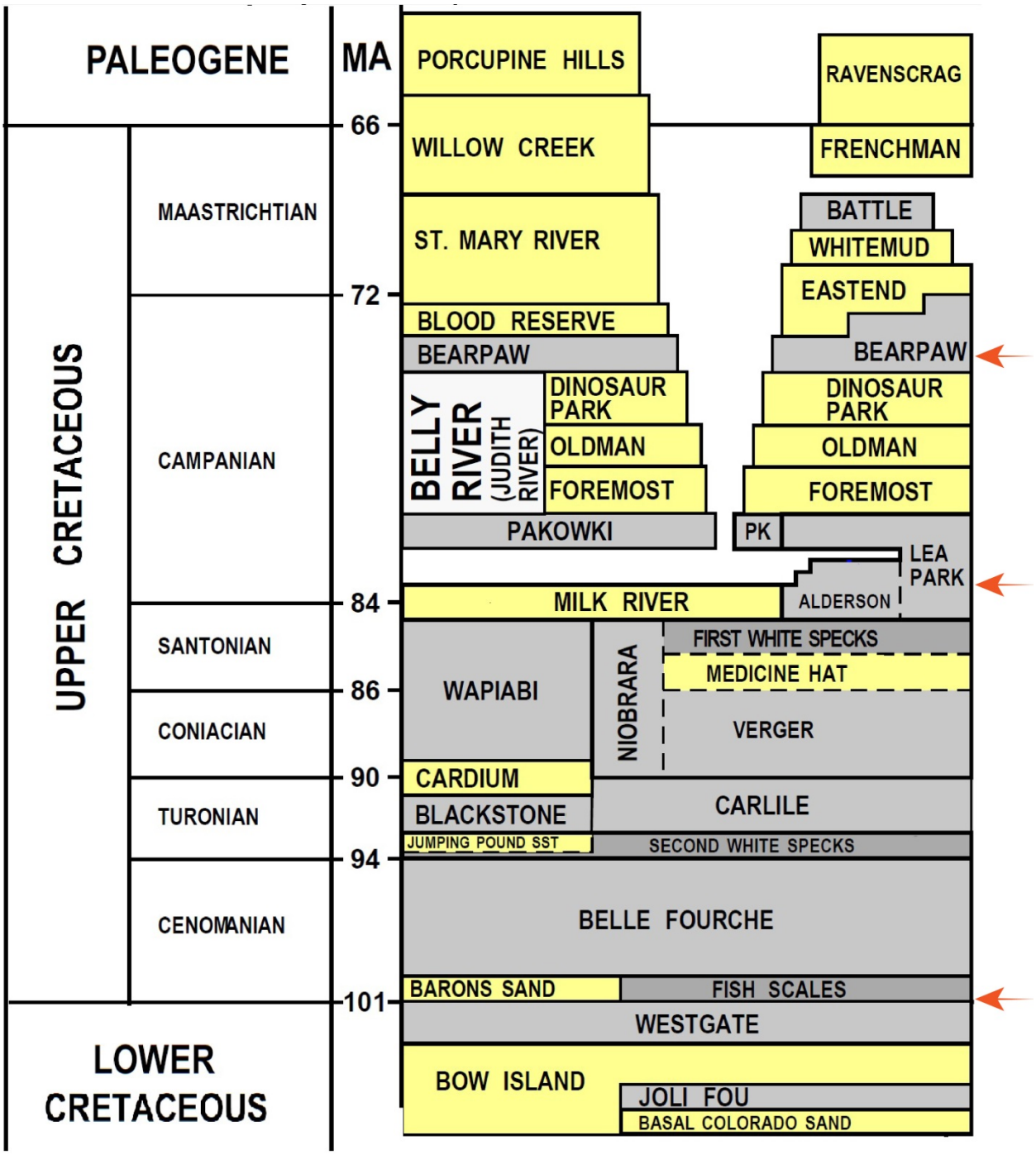

Figure 2. Stratigraphic nomenclature for the study area (modified from Alberta Energy Regulator, 2019). The red arrows indicate the base of the Fish Scales Formation (BFS), the top of Milk River Formation, and the lower Bearpaw Formation flooding surface.

2 Geological Background

The investigated area in southwestern Alberta is part of the Western Canada Sedimentary Basin (WCSB). The WCSB comprises several broad tectono-stratigraphic assemblages deposited over 1.4 b.y. within distinct tectonic settings: (1) The Mesoproterozoic Belt-Purcell Supergroup deposited in an intracontinental rift basin (Price, 1981; Höy, 1992; Evans et al., 2000; Lydon, 2007; Sears, 2007), or an

extensional basin on the western edge of Laurentia with a tectonically active western side (Ross and Villeneuve, 2003); (2) The Late Neoproterozoic Windermere Supergroup was deposited on the initial rifted western margin of Laurentia toward the proto-Pacific Ocean basin (Arnott and Hein, 1986; Hein and McMechan, 1994; Ross and Arnott, 2006). In Alberta, strata of these supergroups are only known in the Rocky Mountain fold-and-thrust belt; (3) The Cambrian to Middle Jurassic assemblages formed in a westward-prograding continental margin terrace wedge that faced the adjacent proto–Pacific Ocean basin (McMechan and Thompson, 1989); (4) The Upper Jurassic to Eocene Cordilleran foreland basin sequence, which overlies the cratonic platform assemblage and accumulated in front of the northeastward-prograding accretionary wedge as the continental lithosphere subsided isostatically under the weight of the advancing wedge, was partly incorporated in, and cannibalized by, the encroaching fold-and-thrust belt (e.g., Price, 1973, 1981; Beaumont, 1981; McMechan and Thompson, 1989, 1992; Stockmal et al., 1997).

Our study area is east of the deformed belt in the Alberta Plains where the sedimentary cover of the North American craton consists of two packages assigned to the depositional settings 3 and 4 defined above. Both packages thicken westward from approximately 3.1 to 6.5 km (see Figure 6 of Lemieux, 1999). The lower package was deposited on a west-facing passive continental margin and consists of a succession of Paleozoic carbonate strata including carbonate ramp, shallow-shelf carbonate, slope carbonate, and reef deposits. The upper sequence was deposited within the foreland basin of the Rocky Mountain fold-and-thrust belt and consists of Upper Jurassic to lower Cenozoic siliciclastic strata derived from the growing orogen to the west. A major unconformity, known as the “sub-Cretaceous unconformity”, more precisely an intra Early Cretaceous time angular unconformity, separates the foreland basin succession from the underlying passive continental margin strata.

From late Proterozoic until Early Jurassic time, the western edge of North America was a passive margin, and deposition occurred in mainly extensional settings (Monger, 1989; Murphy et al., 1995). Episodes of Paleozoic through Middle Jurassic plate convergence and consumption are limited to the accreted or “suspect” pericratonic terranes (e.g., Monger, 1984, 1989; Struik, 1988) and did not markedly affect ancestral North American rocks in Canada. In the late Middle Jurassic, the region became a foreland basin in front of the growing orogen to the west (Monger and Price, 2002). Between the late Middle Jurassic and early Eocene, the Cordilleran realm was mainly under compression, accompanied at different times by sinistral and dextral transpression (e.g., Evenchick et al., 2007). Late Middle Jurassic to early Eocene deformation resulted in a thick stack of east-vergent, generally downward- and eastward-younging thrust slices in the Rocky Mountain fold-and-thrust belt (Pana and van der Pluijm, 2015). Contraction was succeeded by transtension and extension during the middle Eocene (Evenchick et al., 2007; Gervais et al., 2010; Gervais and Brown, 2011). Our study is focused on the Upper Cretaceous and Paleogene formations (Figures 2–4).

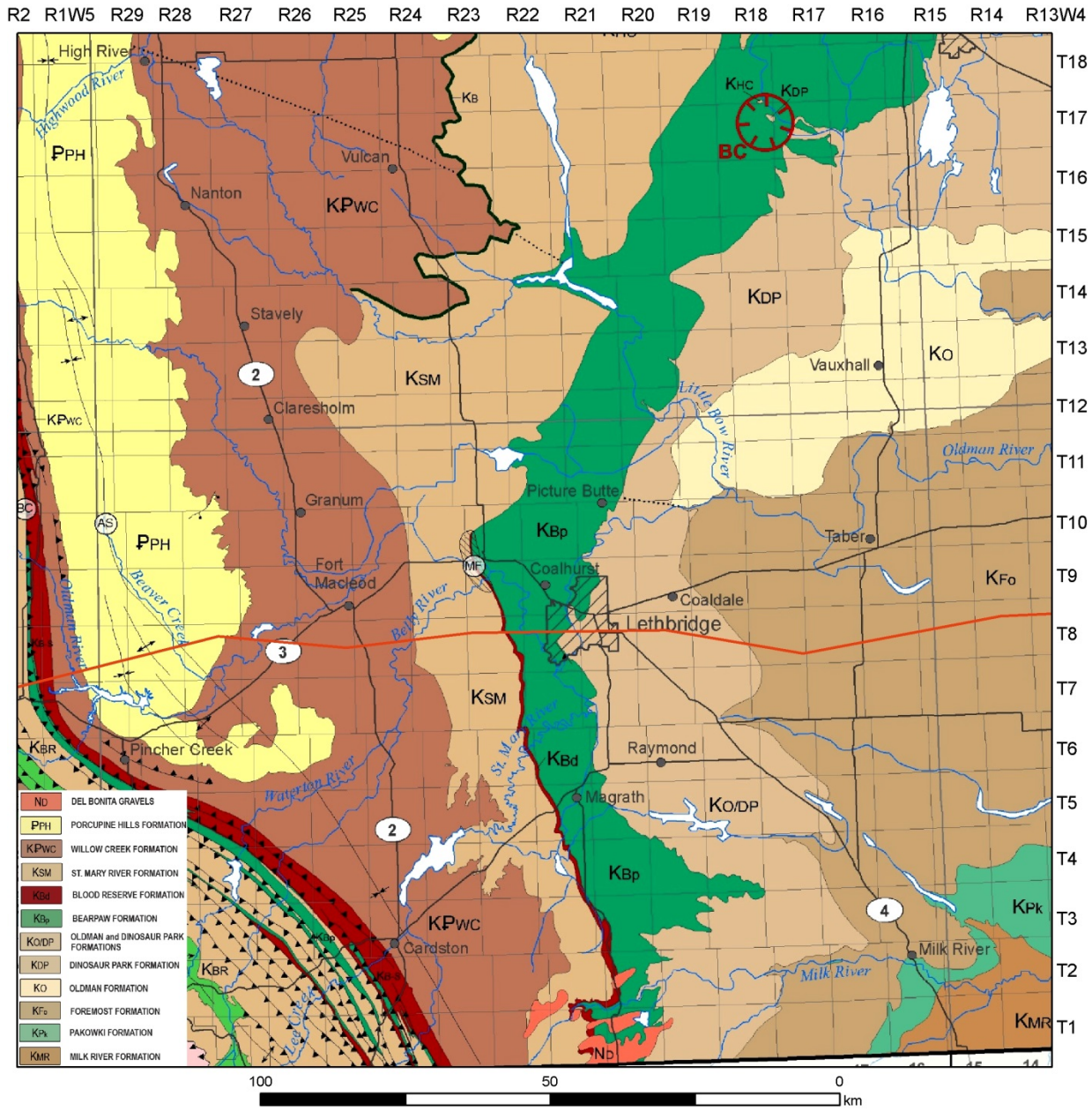

Figure 3. Bedrock geology map of the study area (modified from Prior et al., 2013). The red line indicates the location of the cross-section in Figure 4.

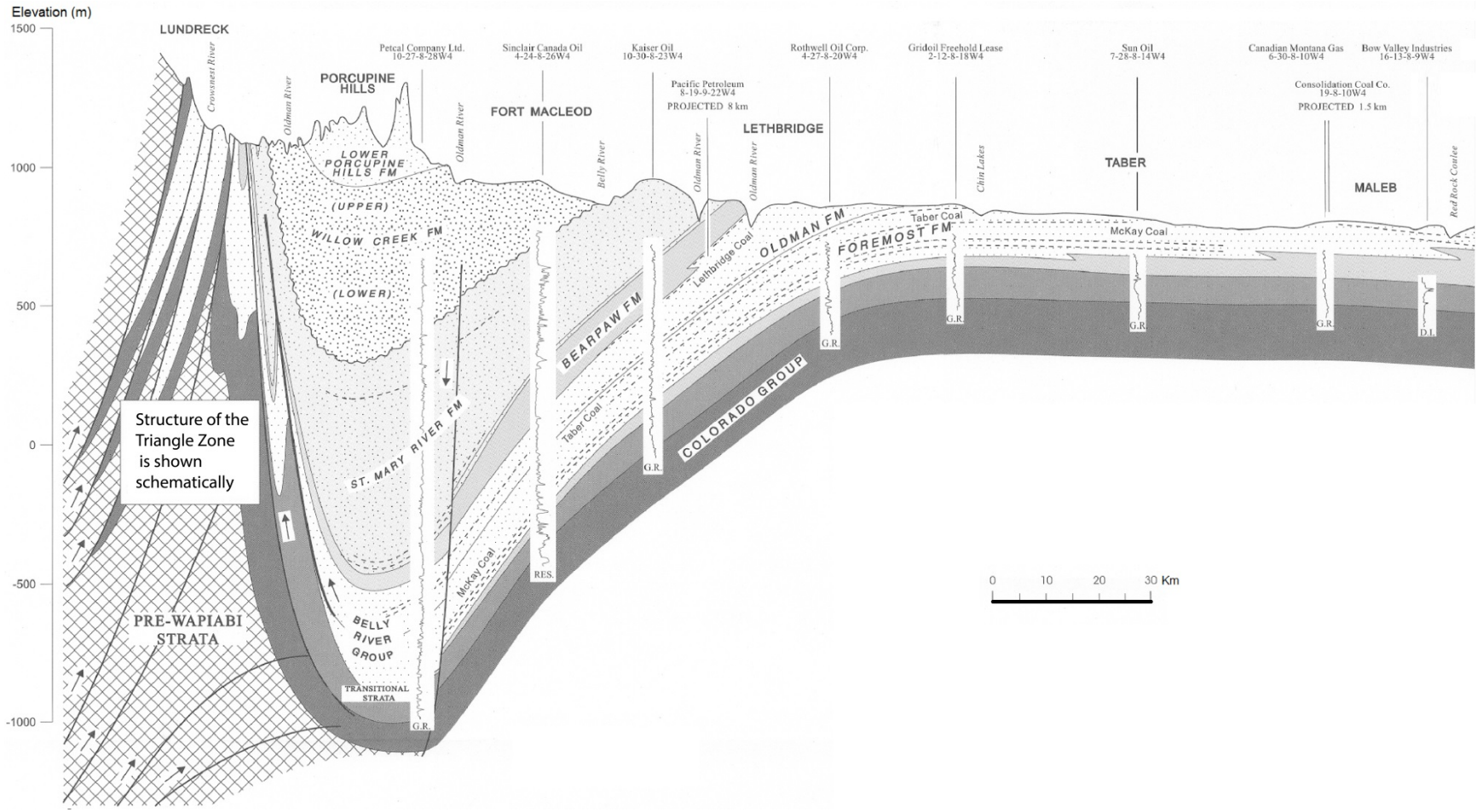

Figure 4. Generalized geological cross-section of the study area (modified from Jerzykiewicz, 1997). The location of the cross-section is indicated by the red line in Figure 3.

From west to east, the structural framework of southern Alberta includes the following three major features: the Cordilleran deformed belt, the Alberta Syncline, and the Sweetgrass Arch. The eastern limit of the Cordilleran deformed belt is marked by the triangle zone (Figure 4). To the east of the Cordilleran deformed belt, the Alberta Syncline is the final expression of the Cordilleran foredeep. The eastern flank of the southernmost portion of the Alberta Syncline, which includes the westerly dipping uppermost Cretaceous and Paleogene Bearpaw, Blood Reserve, St. Mary River, Willow Creek, and Porcupine Hills formations, continues to the east up to the western flank of the Alberta portion of the Sweetgrass Arch. The hinge of the arch is located near the town of Milk River, Alberta, and plunges northeastward, progressively exposing the Upper Cretaceous Milk River and Pakowki formations and the younger Belly River Group from southwest to northeast (Lerand, 1983).

Although the eastern limit of Cordilleran deformation is defined at the triangle zone at the eastern margin of the Alberta Rocky Mountain Foothills, deformation structures have also been reported more than 100 km to the east of the triangle zone in southern Alberta: Russell and Landes (1940) mapped three northwest-striking extensional faults along the banks of the Oldman River near Lethbridge, where the southwestern side was downthrown about 18 to 31 m within uppermost Cretaceous strata of the Belly River Group (Figure 5). Upstream on the Oldman River and about 50 km east of the triangle zone, Irish (1968) identified the north-northwest striking Monarch Fault zone (Figure 5) as a complexly deformed zone of high-angle thrust faults and folds which can be traced at surface for a minimum of 1.5 km across strike (Hiebert and Spratt, 1996). Based on seismic data in the area, Hiebert and Spratt (1996) suggested that the Monarch Fault zone may be the result of displacement inversion controlled by the geometry of pre-existing normal faults in the basement. In an area to the east of Fort Macleod and centred around Twp. 9, Rge. 24, W 4th Mer., Wright et al. (1994) recognized from reflection seismic data several extensional faults, striking from 120° to 128° (Figure 5). These seismically identified faults affected Devonian and Cambrian strata (Figures 3.16, 3.17 of Wright et al., 1994), and are associated with fracturing determined from borehole data in the Mississippian Banff Formation up to the mid-Cretaceous Fish Scales Formation rocks. In the subsurface, duplexing and imbrication structures were also reported to occur up to 65 km to the east of the triangle zone within the foreland basin of southern Alberta (Skuce et al., 1992; Hiebert and Spratt, 1996).

Based on high-resolution aeromagnetic anomaly data acquired over the Phanerozoic Western Canada Sedimentary Basin and the underlying Archean Medicine Hat Block of southern Alberta, Ross et al. (1997) recognized a series of northwest-striking linear anomalies up to 30 km long between the towns of Milk River and Lethbridge, and a set of north-northeast-trending anomalies south of the city of Medicine Hat, with the source of the anomalies located within the sedimentary column at depths of about 250 m or less. Ross et al. (1997) interpreted these anomalies as representing dyke-like igneous bodies possibly correlative with mafic potassic dykes of Eocene age exposed in the Sweet Grass Hills of southern Alberta and northern Montana, which record an increment of post-Cretaceous extension.

Lemieux (1999) studied the Lithoprobe Southern Alberta Lithospheric Transect (SALT) data (Hope et al., 1999) in southernmost Alberta and identified five Late Cretaceous extensional faults (Figure 5), located between ~52 km and ~140 km east of the Cordilleran triangle zone. The westernmost fault (F1) was interpreted as a west-dipping compressional fault and the remaining faults (F2 to F5) as down-to-the-west extensional faults. The extensional faulting in southern Alberta was interpreted to be caused by the flexural subsidence of the foreland triggered by Laramide loading in the adjacent Rocky Mountain fold-and-thrust belt. The thrust displacement on the west-dipping F1 was interpreted as fault inversion shortly after its down-to-the-west extensional development as a far field effect of continuing Laramide compressional stresses (Lemieux, 1999).

Based on interpretation of aeromagnetic, gravity, and well-log data, Berger and Zaitlin (2011), Zaitlin et al. (2011) and Berger and Mushayandevu (2013) mapped a series of graben and half grabens interpreted to have formed during Devonian and Mississippian wrench tectonics related to the Antler orogeny.

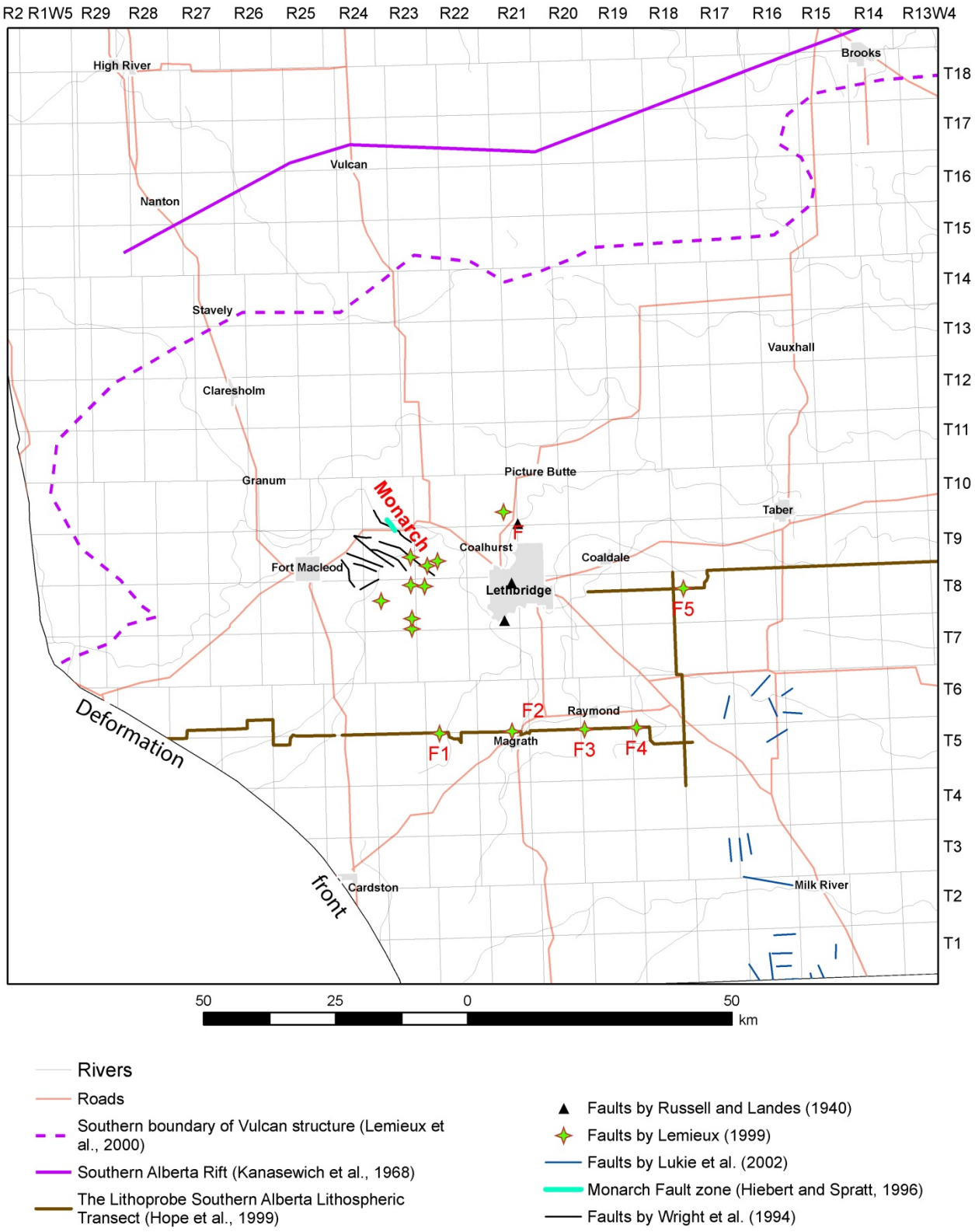

Figure 5. Previously reported structures in the study area.

The faults continued to be active during Triassic and Jurassic extension followed by the formation of the foreland basin. The regional strike of these structures appears to be NW–SE, which corresponds to the trend of magnetic fabrics within the underlying Archean Medicine Hat Block. This NW–SE structural fabric was interpreted to be crosscut by a number of NNE–SSW oriented shear zones (probably related to Laramide compression). In addition, the Vulcan magnetic low, a major basement feature with controversial tectonic significance, may have acted as a zone of weakness, active throughout the tectonic history of the basin (Zaitlin et al., 2011; Berger and Mushayandevu, 2013). The previous work, as mentioned above, forms the basis of our study. Knowledge about the previous mapped faults allows us to verify and constrain our geostatistical analysis of well-log data.

3 Data and Sources of Error

Picks of the tops of stratigraphic units were used as the data for geometric and structural modelling. A stratigraphic top pick in a well is a point defined in three dimensions where the wellbore intersects the top surface of a stratigraphic unit. IHS Markit's PETRA™ software was used for analyzing geophysical well logs and for making picks of the sub-Cretaceous unconformity and other Paleozoic and Cretaceous stratigraphic unit tops. As with other well-log software, when a surface is picked on the geophysical well log, the measured depth of the pick is automatically recorded. The measured depth represents the distance along the wellbore path from the kelly bushing (KB) on the drilling platform to the surface of interest. In a vertical well, the measured depth of the pick is the same as the vertical depth from the KB, and the x, y location of the pick is the same as the wellhead location. When a well is deviated, the measured depth (MD) along the wellbore is greater in value than the vertical depth of the pick; the x, y location of the pick is also different from that of the wellhead. In making stratigraphic correlations and structural maps, it is the elevation of the pick that is used. The elevation of a pick in a vertical well is calculated by taking the elevation of the KB and subtracting from it the MD of the pick. In a deviated well, the x, y location and vertical depth of the pick can be calculated if the deviation survey data are available. In this report, deviated wells without deviation survey data were excluded.

The BFS is easily recognizable by a sharp increase in gamma-ray log readings. The top of Milk River Formation is easiest to recognize on resistivity logs and typically recognizable on SP, sonic, density, and porosity logs. The lower Bearpaw Formation flooding surface is characterized by a widespread, consistent resistivity and gamma-ray log pattern that represents the first regionally correlative flooding surface above the Belly River Group. Each of the three surfaces is associated with a distinctive deflection on geophysical well logs and, thus, can be picked consistently. For this report, we have used 4880 picks for the lower Bearpaw Formation flooding surface, 9591 picks for Milk River Formation, and 17 553 picks for the BFS. The picks for the lower Bearpaw Formation flooding surface were picked by the first author for all the wells with digital logs found in the study area. Picks for Milk River Formation include those published by Glombick and Mumpy (2014), and additional picks made by the first author. The majority of picks for the BFS were compiled from various AGS sources, with additional infilling and refined picks made by the first author during geostatistical analysis and geological modelling.

The first source of uncertainty in the elevation of picks is the potential error found in the elevation of the KB, from which the pick elevation is calculated. The error in KB can be caused by errors in surveying the ground elevation of the well site, because the KB elevation is usually derived from adding the height of the drilling platform above the ground surface to the surveyed ground elevation.

The second source of error is the uncertainty in well location. In western Canada, wells are licensed based on the bottomhole location, and the coordinates that define the location were based on a survey grid that was tied to known markers. In Alberta, the grid used by the petroleum industry is the Alberta Township Survey version 4.1 (ATS 4.1). The ATS grid has gone through several revisions, and each revision has resulted in corrections to previously derived grid points. The accuracy for the ATS 4.1 is ±3 metres. The surfacehole location is first defined as metes and bounds based on the ATS grid, which are the offsets relative to the southeast corner of the section in a township. The bottomhole location is calculated based

on the directional survey from the surfacehole coordinates. Some uncertainty in well location is inevitably introduced in these calculations and conversions and will translate into uncertainty in the elevation of formation-top picks.

The third source of error is human error and typically results from inconsistent or incorrect placement of picks on well logs. This can be partly caused by using inconsistent interpretation/correlation models (lithostratigraphic/layer-cake versus sequence stratigraphic; see Tinker, 1996, for example), limited availability and poor resolution of logs, and complexity in facies changes. Other potential sources of error include data-entry mistakes and incorrect well-log depth calibration.

The errors associated with picks cannot be completely eliminated; however, they can be reduced and managed to an acceptable level (see Section 4.1 below).

4 Methodology

After deposition, sedimentary units may undergo regional compaction, regional deformation, and local structural disturbances. In the Alberta Basin, local structural disturbances may be related to differential compaction over reefs, karst development, salt dissolution collapse, faulting, impact craters, and glaciotectonics, to name a few. Consequently, the present-day elevation of a stratigraphic unit top may represent the combined effects of both the regional and local processes. The objective of this study is to map potential subsurface bedrock structures by highlighting and separating the offsets caused by local deformation (faults) from the combined effects of regional deposition, deformation, and compaction. The methodology used in this study was first developed by Mei (2009) and allows recognition of metre-scale formation-top offsets that are below the detection or resolution limits of conventional seismic surveys.

In the Alberta Basin, local structural features are represented by bedrock surface undulations or roughness; this is because the difference in the elevation of a bedrock surface caused by local features is at a much smaller scale than that caused by regional deformation. To highlight the local structures, a regional trend surface is first modelled to account for the combined effect of the regional processes including tilt of the basin towards the orogen or regional arches. Then, the trend is removed from the data and simple kriging is applied to the residuals to account for the local variations using ArcGIS Geostatistical Analyst. The local structures are thus highlighted in the resultant residual map.

Marine flooding surfaces are preferred for mapping formation-top offsets in this study because: 1) they are smooth (not necessarily flat) after deposition, approximating a flat-lying datum, 2) they are regionally extensive, 3) they typically have a distinct log signature and can be picked on well logs easily and consistently, unlike the more variable nonmarine bedrock surfaces. Marine flooding surfaces have remained smooth, possibly with wide undulations, after regional compaction and deformation; they become disturbed only after they are offset by local structural features (e.g., faults and draping folds). As a result, local structures with a relatively high differential of pick elevations can be highlighted after removal of the regional, very low-gradient structural features of the basin, such as the regional dip towards the orogen.

4.1 Data Cleaning and Refinement

In addition to the regional basin architecture that may mask the local structures on bedrock surfaces, the errors associated with the formation-top picks also tend to blur the local structures. If the picks were error free, the interpolated bedrock surface would be smooth except where it is offset by local structures, making the local structures easily identifiable. Using the methodology described above, the variations captured in the residual map after removal of the regional trend are represented by undulations caused by both local structural features and errors that are propagated into the process of making picks and generating the bedrock surface. These errors need to be identified and reduced where possible in order to best highlight the local structures.

The data cleaning and refinement process includes the following steps (Mei, 2009):

1) A local trend surface was generated around each data point using the surrounding data points; then, the deviation of the data point from the local trend was calculated.
2) The histogram of deviations was examined and the data points with deviations larger than an initially determined threshold (e.g., two or three standard deviations away from the mean deviation) were identified as outliers.
3) The outliers were then visually examined against the structure map and grouped into two categories based on their distribution patterns. One category contained outliers that were clustered in a linear or circular pattern, potentially indicating local structural features. The other category contained outliers that were randomly distributed across the study area, likely representing erroneous picks.
4) The outliers were then examined against well logs to confirm the existence of local structures or to correct other errors. Data points identified with KB errors are corrected or refined with available digital elevation model (DEM) data (e.g., light detection and ranging or Shuttle Radar Typography Mission DEM), or using the offset well KBs in a flat area. The data points associated with picking errors were reassessed. Wells with errors that were undetermined or could not be corrected (e.g., lack of good quality logs for re-picking) were removed from the analysis.
5) The steps mentioned above were repeated until a minimized and acceptable degree of uncertainty was reached. The rule of thumb is that the standard deviation should be less than, ideally, half of the magnitude of the offset to be targeted, or the typical vertical throw of faults in the study area, which usually can be found in previous publications.

4.2 Mapping Structural Features

To define a structural feature in three-dimensions, the analysis needs to be applied to multiple bedrock surfaces. This also allows for structural features to be differentiated from each other based on the following characteristics:

- Faults: showing linear pattern of offsets (not all linear features/offsets are faults).
- Salt-dissolution sinkholes and collapses: circular features variable in shape and size and containing offset/disturbance that may be traced through the entire Cretaceous succession down to the responsible Devonian evaporite beds if data are available.
- Glacial deformation: variable in shape (faults and thrusts) and with offset/disturbance limited to surficial deposits and near-ground-surface bedrock.
- Impact structures: circular features with offset/disturbance having the potential to affect considerable depths of strata and recognized by diminishing influence/offset with increasing depth, depending on original depth of target rocks.
- Volcanic structures: circular offset/disturbances that can be traced throughout the entire sedimentary cover.

To identify offsets that could potentially be related to faults, the cleaned data points were used to model a regional trend surface using the local polynomial interpolation technique in ArcGIS Geostatistical Analyst (Mei, 2009). The trend was subtracted from the data points, and a residual map was created to accentuate the local linear offsets using simple kriging. The resulting linear offsets were then verified using well logs, well cross-sections and other previously published data.

The accuracy of the location of the highlighted offsets is dependent on the well-log quality and well spacing. The uncertainty in the amount of vertical throw is managed by the quality control process as described in the preceding section. In addition, the analysis used in this study inherently smooths out random errors or noise because the interpolation used is a weighted-averaging technique and, thus, has a smoothing effect (see the following for detailed explanation). The residuals are found normally distributed with few exceptions, and the residual surface is interpolated using weighted-averaging

techniques. The interpolated residual surface is a surface of interpolated local means. The uncertainty of the mean value of a normal distribution (the residuals in this case) is measured by the standard deviation of the mean (SDOM), or standard deviation in reference to a mean value, which is calculated as $\pm\frac{\sigma}{\sqrt{n}}$, where σ is the standard deviation of the data, and *n* is the number of data values used in the neighbourhood of the interpolation. The SDOM is often used as a measure of the precision of measurements and is much smaller than the standard deviation of the entire data points used. It has been proven that there is about a 66% probability that the true mean will lie within $\pm\frac{\sigma}{\sqrt{n}}$ of the mean, and about a 95% probability that the true mean will lie within twice this distance from the mean value (Taylor, 1997), as the mean value of a normal distribution is also normally distributed. The weighted-average interpolation, used in creating the residual surface, inherently removes much of the noise in the data and leads to accentuation of local structures in the residual map.

4.3 Initial Characterization of Offsets

The offset mapping method, as described in the preceding sections, was applied to multiple formation tops to: 1) increase the level of confidence of results when a linear offset pattern is identified in multiple horizons, and 2) allow potential faults to be characterized in three dimensions, as opposed to treating a fault as a linear feature on a two-dimensional map.

The method was also applied to formation-thickness data to: 1) increase the level of confidence when a linear offset pattern can also be recognized from isopach maps, and 2) determine whether the potential fault is syndepositional or postdepositional. A syndepositional fault is accompanied by changes in thickness across the fault. An isopach for each interval was deconstructed into two components: "regional" versus "local" subsidence, using the same method described in Section 4.2. The local subsidence map can be compared with the linear offset map derived from formation top picks. If the local subsidence or isopach remains consistent across the linear offset pattern, it suggests that the offset is postdepositional, whereas local subsidence changes across the linear offset pattern, suggests that the offset is likely syndepositional.

4.4 Comparison with Conventional Methods

The conventional approach to subsurface structural mapping in the WCSB used information from well-log data to construct contour and isopach maps (e.g., Lukie et al., 2002) and well-log cross-sections, and has achieved varying success in detecting structures and faults with offsets in the range of tens to hundreds of metres. One of the problems with using well-log data is that one cannot routinely discriminate formation-top offsets in the range of metres because they are beneath the resolution of the technique. The structure and isopach contour maps are usually dominated by a regional trend and this trend commonly masks the small-scale, fault-related formation-top offsets. Consequently, much of the information on faults associated with small offsets remains unnoticed in the well-log data.

The well-log cross-section method uses a string of wells for identifying the offsets it crosses. When the offset is small and the wells used are widely spaced (e.g., on average one well per township or about 10 km), it is difficult to determine whether the change in elevation of a formation top is due to natural undulation or caused by a fault; as a result, multiple cross-sections, ideally orthogonal to the strike of the linear offset, are necessary for confirming the offset. The more cross-sections are used, the higher the level of confidence in detecting the offset. Also, multiple cross-sections are required to define the location of the path of a fault along the strike. The method used in this report uses all the data points on one side of a linear offset and all the data points on the other side of the offset to establish the systematic and small-scale offset between the two blocks on each side of the linear offset. It is similar to the well-log cross-section method using multiple cross-sections, but is more effective and accurate in determining the offset and strike path of a potential fault because it analyzes all the data points on either side and at some distance from the potential fault.

Another commonly used method for fault detection uses seismic reflection data. The vertical resolution of conventional seismic reflection data is limited to approximately one-quarter of the dominant wavelength (Sheriff, 1991). For the SALT data, vertical resolution translates to approximately 30 m, using a dominant frequency of 35 Hz and an average velocity for the sedimentary sequence of 4500 m/s (Lemieux, 1999). As a result, thin beds and fault displacements of 30 m or less are not resolvable on the seismic profiles from SALT data. In other words, migration may image the smaller offsets in strata as smooth, continuous reflections. Deformation in the shallow part of the sedimentary section over the master fault may be more distributed, and, therefore, resolved as folds rather than a discrete fault, and these extensional forced folds imaged may actually represent secondary extensional and reverse faults with smaller offsets, as modelled by Withjack et al. (1990) using single- and multiple-layer clay models. Also, the structures must have a dip of less than 70 degrees to be properly resolved seismically. However, the method used in our study overcomes this limitation and allows for detection of offsets with a vertical throw as small as 5 m (see Sections 4.1 and 4.2; Mei, 2009). The combination of our methodology and seismic profiles allows us to tackle very small vertical offsets through the sedimentary cover, which may represent faults with minor displacement.

Trend surface analysis (TSA) has been widely used for analyzing geological data and highlighting local structures (Grant, 1957; Wren, 1973). TSA uses global polynomial of best fit to the data for trend modelling (Baird et al., 1971; Davis, 2002). The trend in the conventional TSA is primarily a computer-controlled model because only one parameter, the power value of the polynomial regression, can be input for trend modelling. This method does not allow geologists to constrain the trend by inputting geological knowledge in the modelling. The analysis used in this study is a refined TSA and uses local polynomial or kriging to model the trend (Mei, 2009). Figure 6 shows an example of the modelled trend for the lower Bearpaw Formation flooding surface. It shows a regional trend dipping from the east to the west. Superimposed on this trend are subregional, gently undulating features; among them are a high in the area in Twp. 1–4, Rge. 20–25, W 4th Mer., which is related to the Sweetgrass Arch, and a low located in the area in Twp. 14–16, Rge. 24–26, W 4th Mer., which overlaps the Vulcan magnetic low. These gently undulating regional dip and subregional features, which are not the direct interest of the offset mapping, are included in the trend and, thus, removed with the trend in the subsequent analysis. As a result, the local, targeted structures can be best highlighted in the residual map (Figure 7).

5 Results and Interpretation

A residual map was used to first locate an approximate location of an offset lineament, and the final location was then determined by examining the data values along the lineament and placing the lineament between the points with the greatest and/or consistent difference in elevation. When the interpreted lineaments are displayed on the residual map, some lineaments may be found in areas with the same colour across the lineaments, due to the inherent smoothing effect in the map and the type and resolution of the colour rendering method selected. Numerous linear offsets have been identified from the lower Bearpaw Formation flooding surface (Figure 7), Milk River Formation top (Figure 8), and BFS (Figure 9). These lineaments appear to strike NW–SE, except in the southeastern portion of the study area, where the linear offsets strike NNW–SSE. In addition, these NW–SE offsets appear to be crosscut and possibly displaced by a number of shorter NE trending lineaments/zones (Figures 7–9). In addition, a circular astrobleme structure in Twp. 17, Rge. 17–18, W 4th Mer., first recognized by Glombick et al. (2010) using the method mentioned above, was highlighted from the lower Bearpaw Formation flooding surface (Figure 7) and the Milk River Formation top (Figure 8); it becomes less obvious with increasing depth and is represented by a subtle depression on the BFS surface.

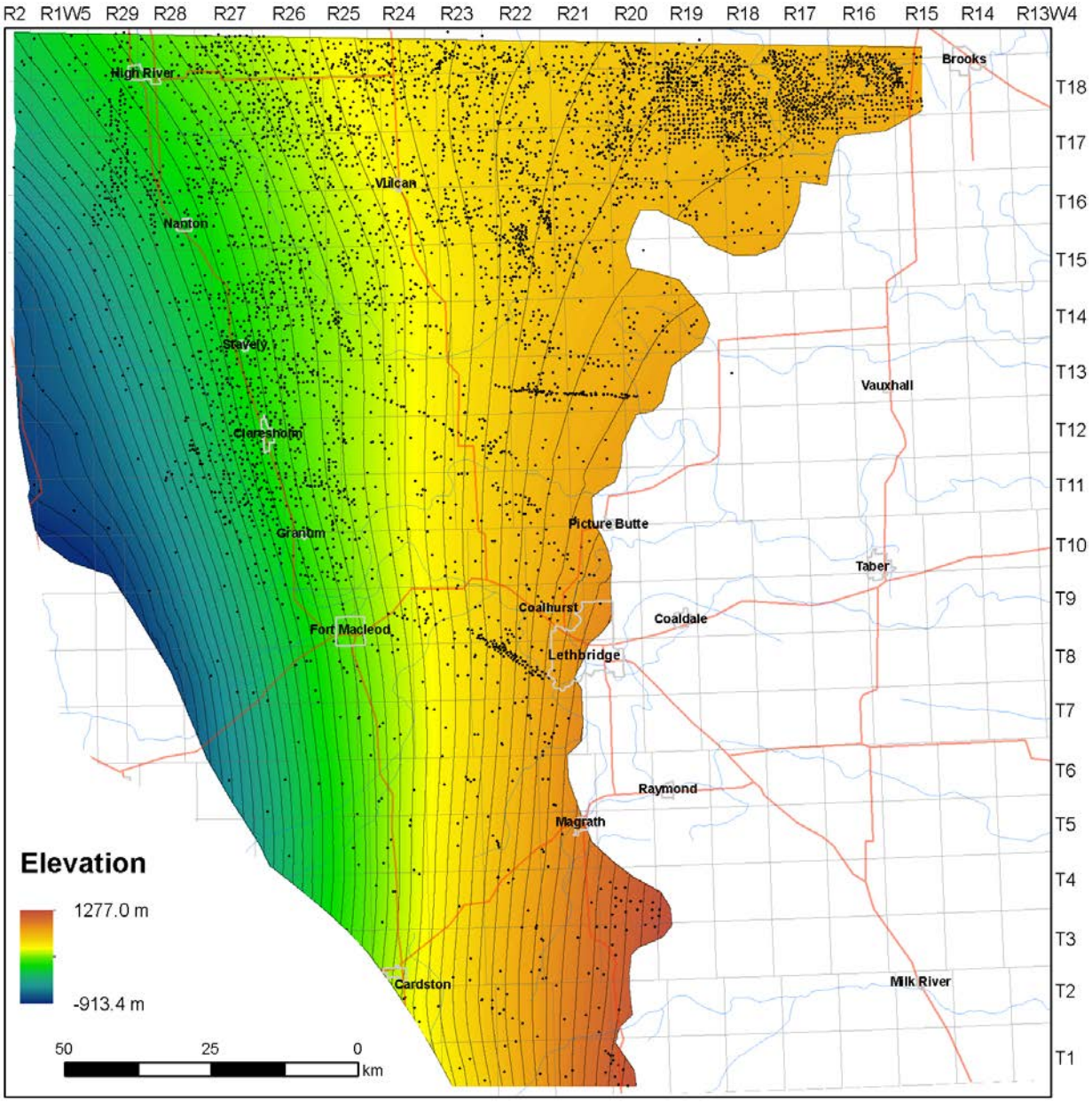

Figure 6. The trend surface modelled for the lower Bearpaw Formation flooding surface, clipped to the erosional edge to the east, and the data limit and deformation front to the west. Black dots indicate control wells and black lines are contour lines with an interval of 50 m.

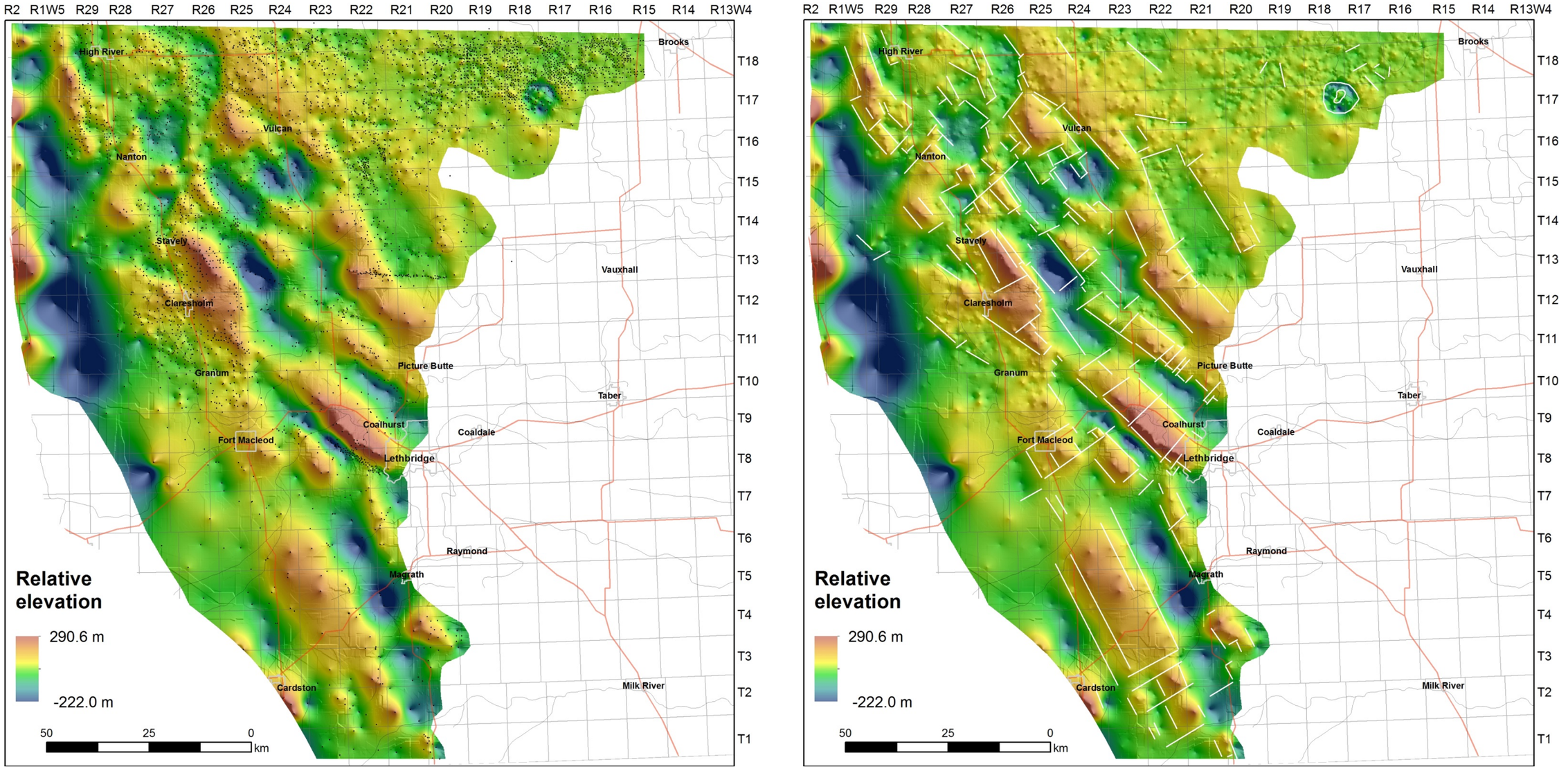

a) b)

Figure 7. Residual map of the lower Bearpaw Formation flooding surface, clipped to the erosional edge to the east: (a) includes control wells and (b) map of (a) with interpreted offsets (white lines).

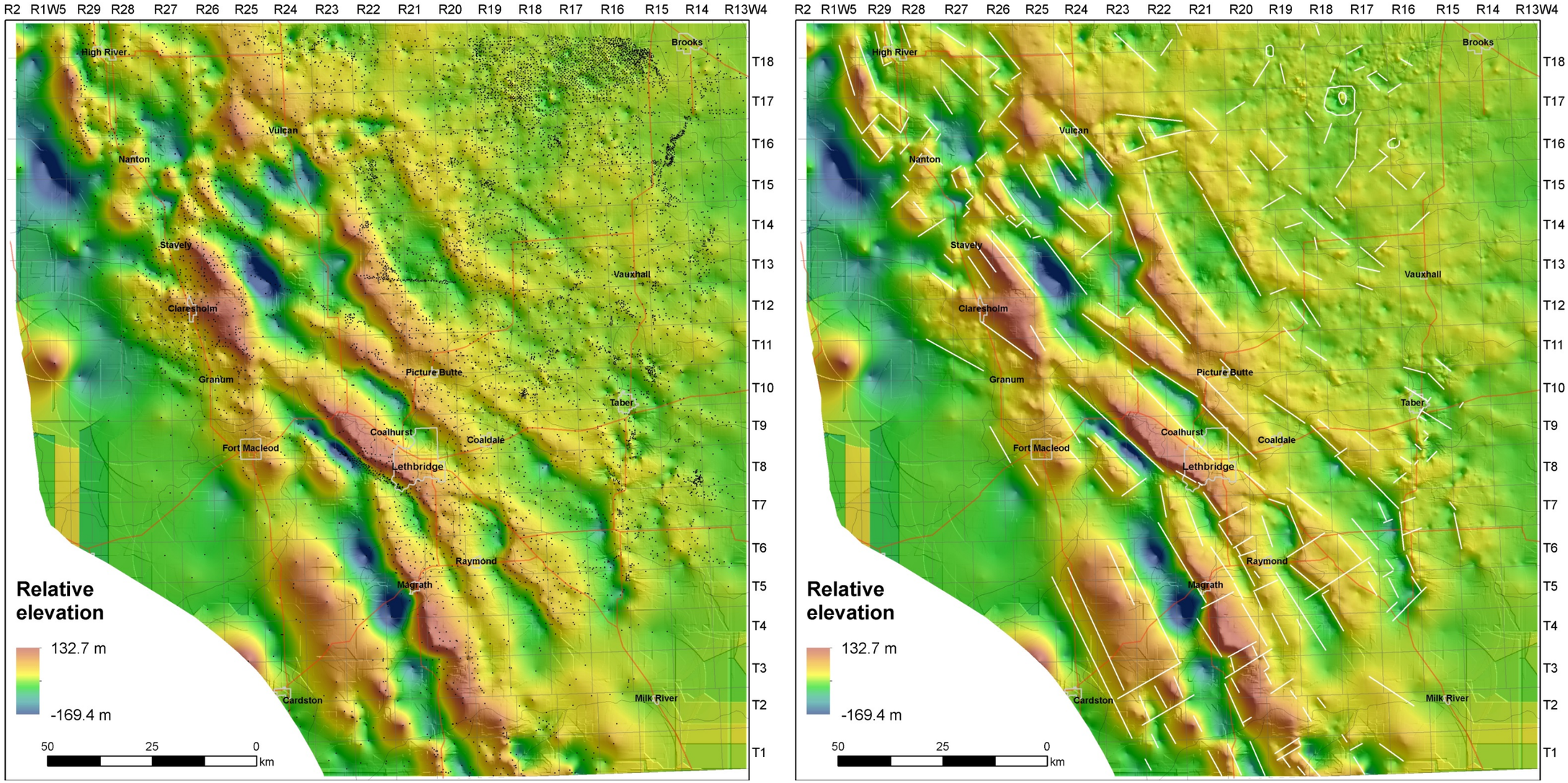

a) b)

Figure 8. Residual map of the Milk River Formation top in the study area: (a) includes control wells and (b) map of (a) with interpreted offsets (white lines).

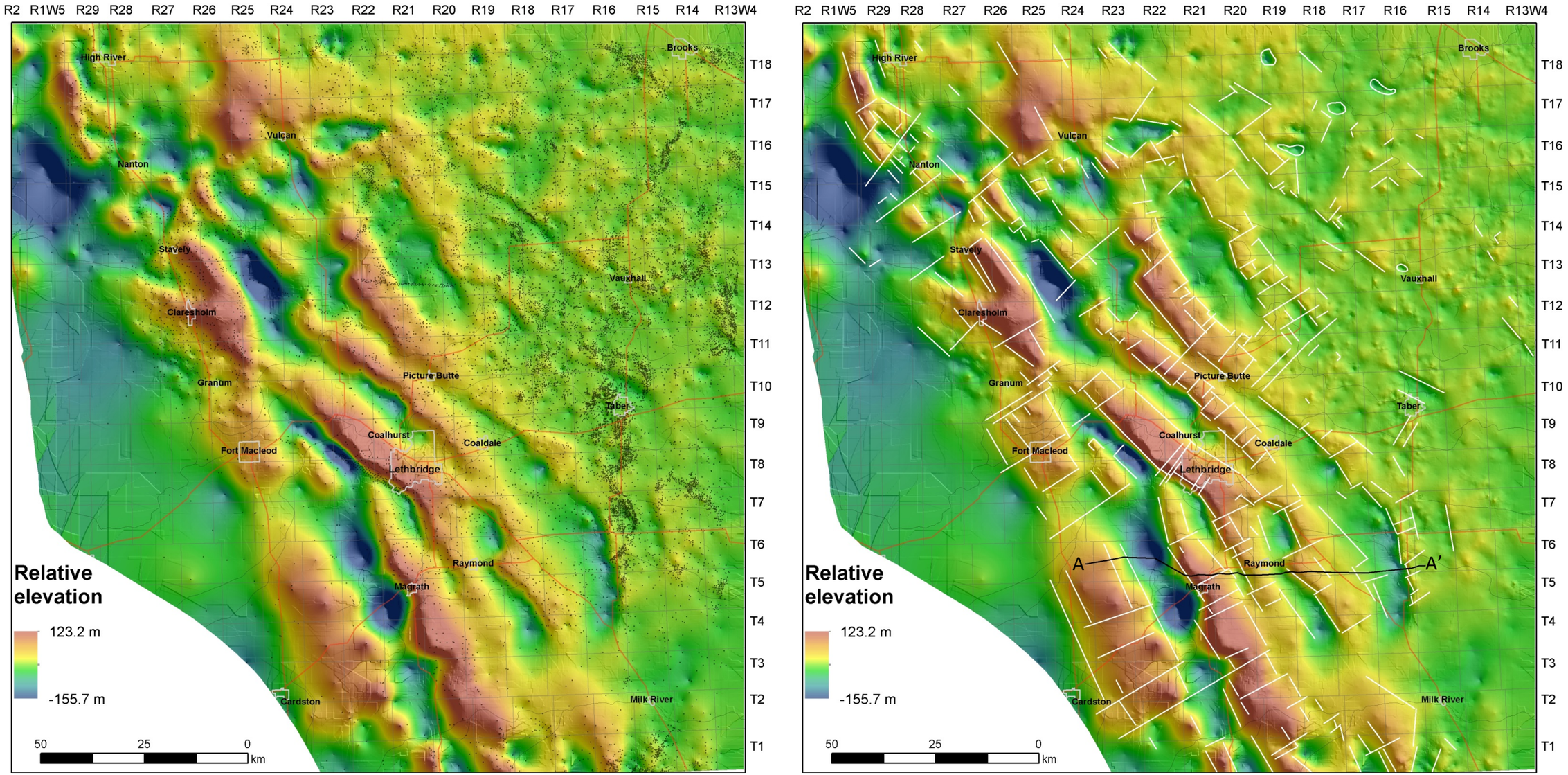

a) b)

Figure 9. Residual map of the base of the Fish Scales Formation (BFS) in the study area: (a) includes control wells and (b) map of (a) with interpreted offsets (white lines). The black line in (b) indicates the location of the cross-section shown in Figure 10.

Some of the linear offsets recognized from these surfaces were validated with selected well logs across the lineaments; this is to confirm that the parameters used in the method to map the offsets for the entire study area is effective. Figure 10 shows an example of a cross-section traced across faults F1, F2, F3, F4 and possibly the southern extension of fault F5 of Lemieux (1999). It also shows the log characteristics of selected surfaces.

Figure 11 shows an isopach map for the interval from the BFS to the top of the Milk River Formation. The isopach map was created to assess whether the interpreted linear offsets represent syndepositional growth faults. By comparison of the offsets and the isopach map, a syndepositional fault can be recognized by the thickness difference of a given stratigraphic unit across the fault.

Figure 12 shows all the lineaments interpreted from the lower Bearpaw Formation flooding surface (Figure 7), Milk River Formation top (Figure 8), and the BFS (Figure 9), with the isopach map of the interval from the BFS to the top of the Milk River Formation (Figure 11) as the background map. Many of the linear offsets interpreted from the three surfaces coincide very well with each other, suggesting that these offsets impacted all the three surfaces. Some of the linear offsets overlap with the lineaments derived from the isopach map, suggesting that they may represent growth faults that accommodated differential subsidence during the deposition of the interval from the BFS to the top of the Milk River Formation. A good example is the area in Twp. 16–17 and Rge. 22–25, W 4th Mer., where the thickness of this interval is clearly greater than in the surrounding areas. This area is bounded by a series of syndepositional or growth faults that have decreasing amounts of offsets from the BFS to the top of the Milk River Formation (compare Figures 9 and 8); the offsets become subtle on the lower Bearpaw Formation flooding surface (Figure 7), which is the shallowest of the three examined surfaces. Interestingly, this area coincides with the Southern Alberta Rift, which was recognized as a Precambrian rift buried beneath the Western Canada Sedimentary Basin (Kanasewich et al., 1968), and defines the northern boundary of the Vulcan low magnetic structure (Eaton et al., 1999; Lemieux et al., 2000).

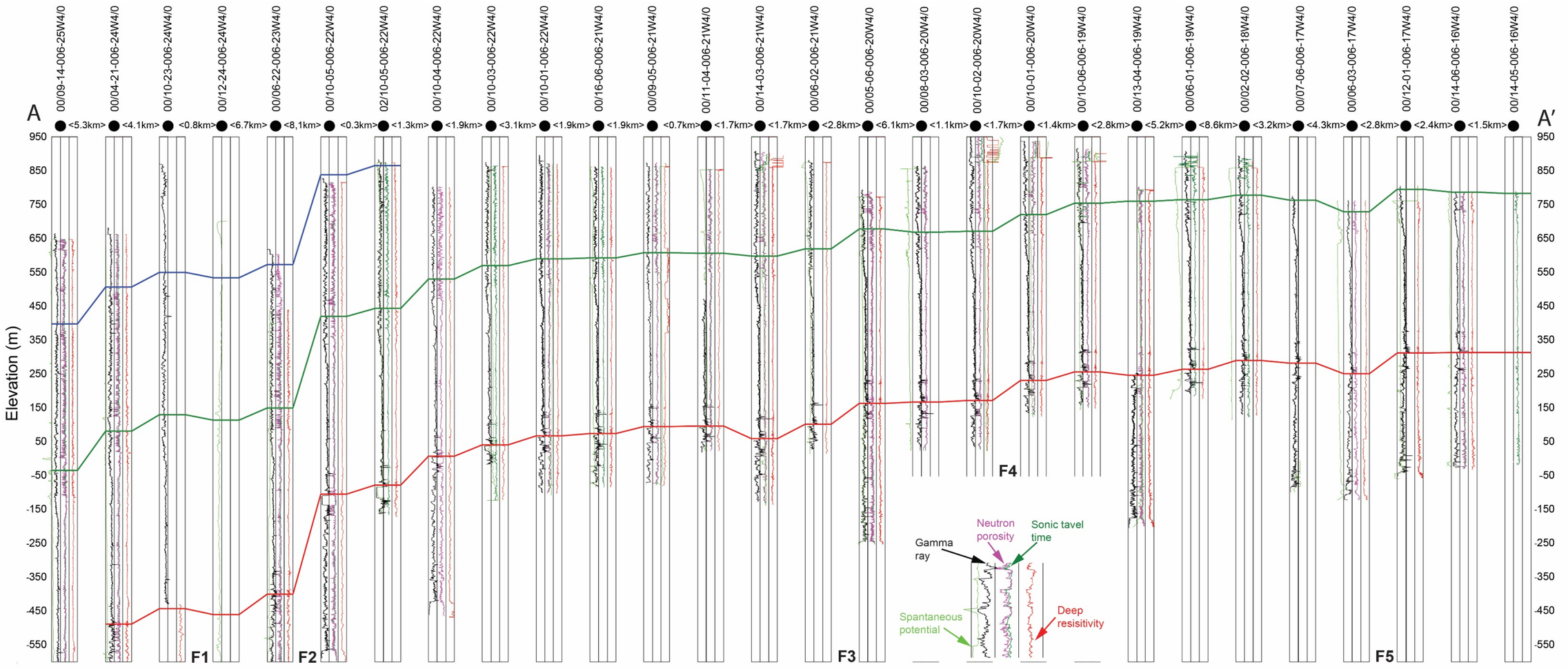

Figure 10. Structure cross-section showing the horizons and log characteristics of the lower Bearpaw Formation surface (blue line), the Milk River top (dark green line) and the base of the Fish Scales Formation (red line), as well as the offsets of faults F1 to F4 and possibly the southern extension of fault F5 of Lemieux (1999). The location of the cross-section is shown as the black line in Figure 9b and the black dashed line in Figure 13 with location of faults F1 to F5.

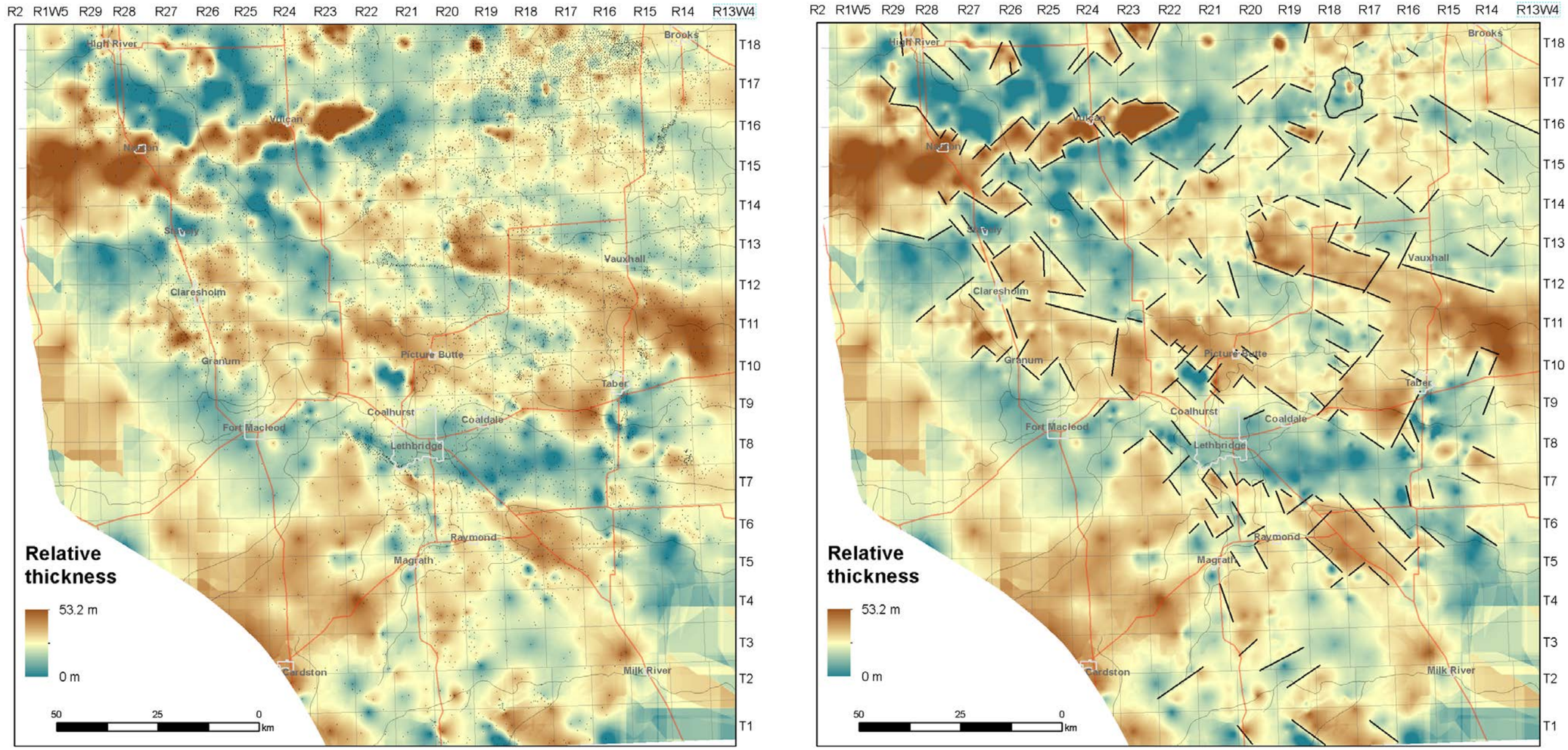

a) b)

Figure 11. Isopach map of the interval from the base of the Fish Scales Formation (BFS) to the Milk River Formation top: (a) includes control wells and (b) map of (a) with interpreted lineaments.

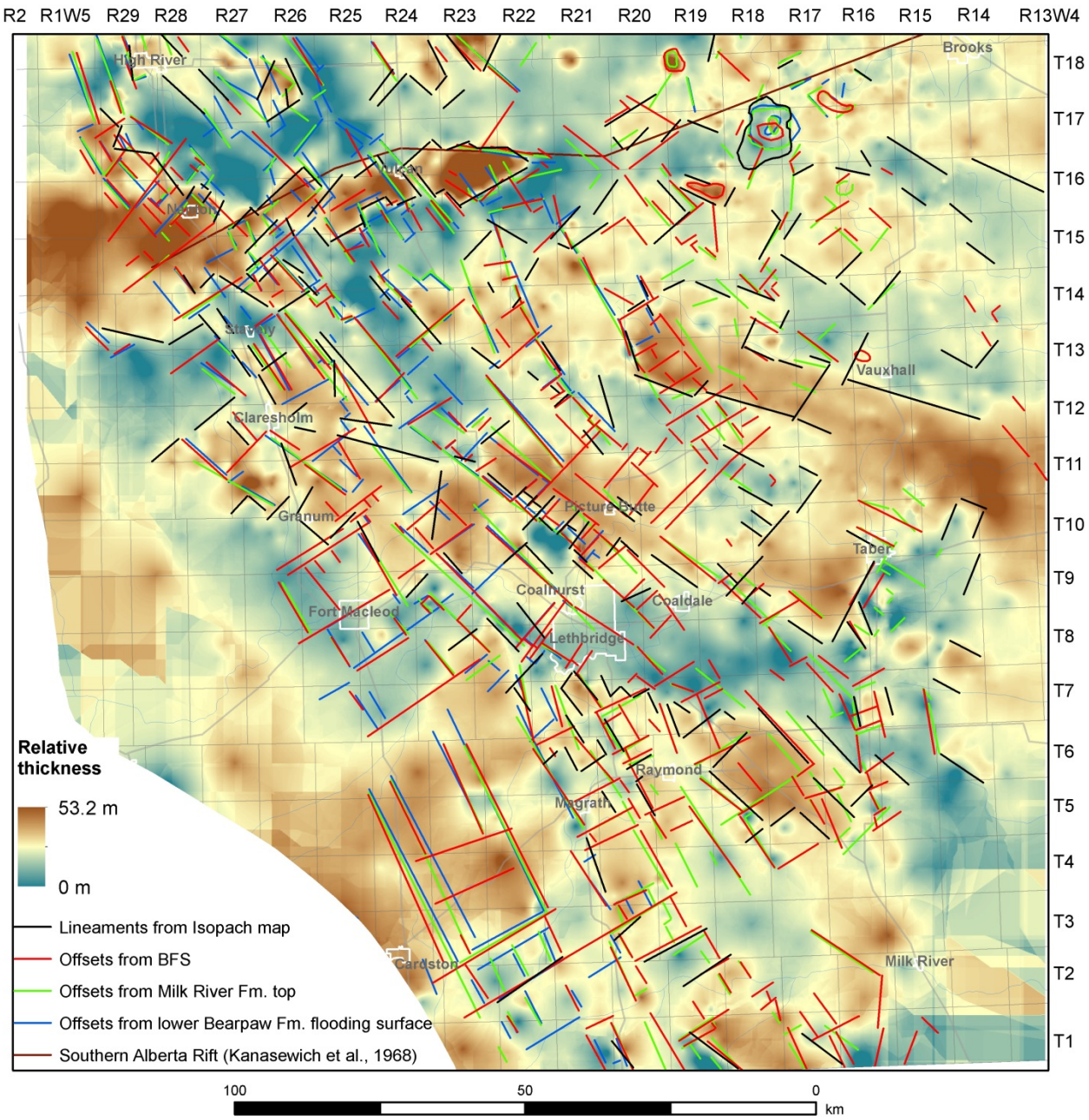

Figure 12. Interpreted offsets from the lower Bearpaw Formation flooding surface, Milk River Formation top, and base of the Fish Scales Formation (BFS) overlain on the isopach map of the interval from the BFS to the top of Milk River Formation (from Figure 11).

5.1 Comparison to Previously Reported Faults

Previously, faults have been identified at isolated riverbank outcrops and locations along the seismic reflection lines of the SALT (Russell and Landes, 1940; Wright et al., 1994; Hiebert and Spratt, 1996; Lemieux, 1999). Figure 13 shows that our offset lineaments mapped from the BFS coincide very well with the previously reported faults. Moreover, our offset maps have revealed the orientation and extent of these faults by recognizing them on multiple geological unit-tops, allowing for a 3D representation (Figures 7–9).

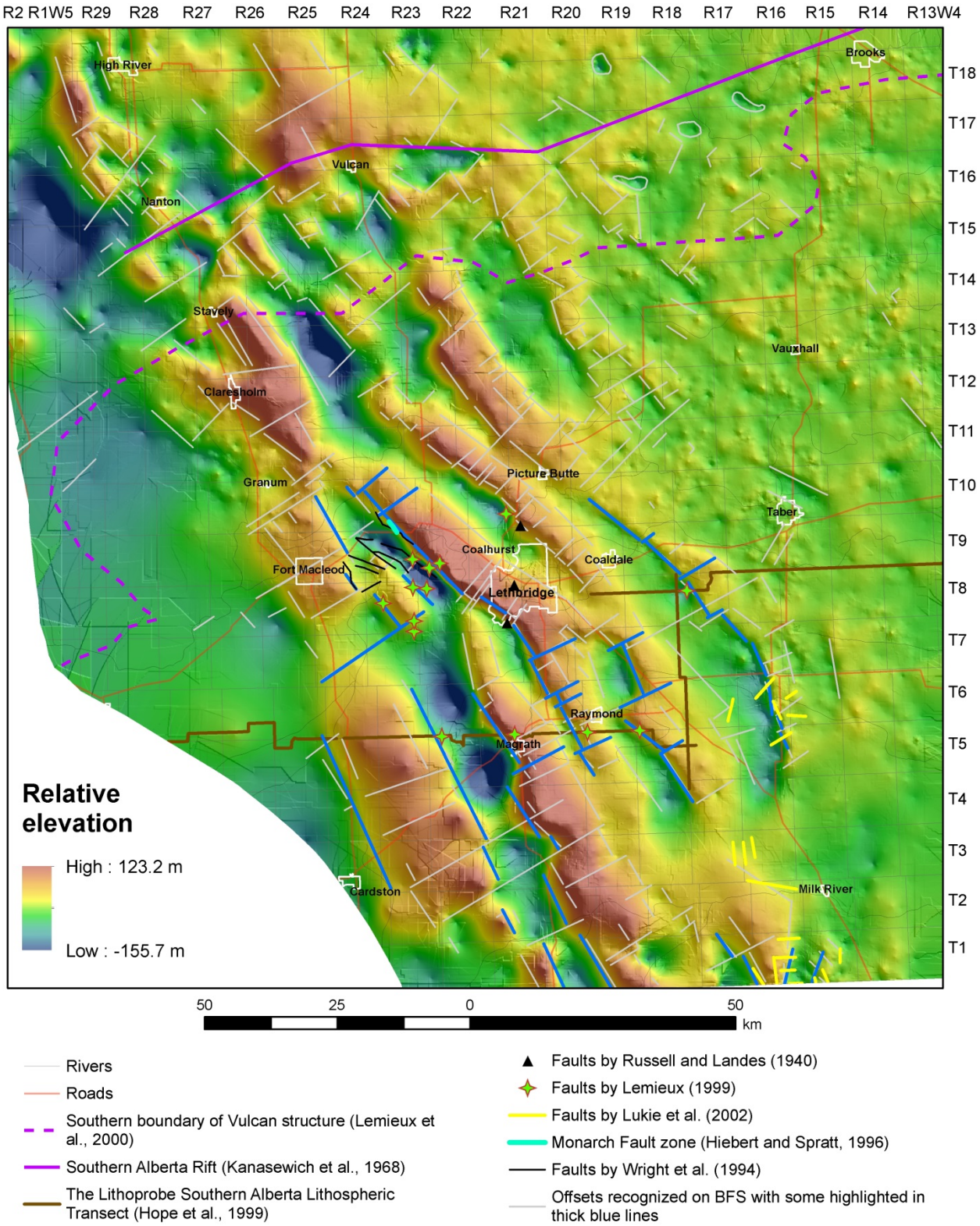

Figure 13. Comparison of mapped subsurface linear offsets with previously reported faults. The background is the residual map of the base of the Fish Scales Formation (BFS).

Lemieux (1999) recognized 5 major faults, named F1 to F5 from west to east, from the seismic reflection profile of the SALT data (Figure 13). Faults F1 to F4 were recognized on the SALT Line 30 that runs along the southern border of Twp. 6 from Rge. 26 to19 W 4th Mer., and fault F5 on the SALT Line 31 in Twp. 8, Rge. 18, W 4th Mer. The F2 and F4 faults show breaks in the near-basement, Cambrian and Devonian reflectors (Lemieux, 1999), and no breaks but folding are observable in reflectors for overlying Mississippian (Livingston Formation), Jurassic (Rierdon Formation), Lower Cretaceous (BFS), and Upper Cretaceous (at least into Belly River Group) (Figure 10). The F5 fault shows a break in near-basement up into lowermost Upper Cretaceous reflectors (BFS) and folding of Upper Cretaceous reflectors (up into the Milk River Formation) (Lemieux, 1999; Figure 10). The folding is interpreted to be extensional forced folding developed above the master down-to-the-west extensional faults, cutting Lower Paleozoic strata (Cambrian and Devonian) with distributed strain in overlying strata (Mississippian, Jurassic, and Cretaceous). The F1 fault is unique in that the hangingwall side (western side) appears to be elevated above regional trend on the seismic reflection profile, and was interpreted as an inverted west-dipping extensional fault that at present displays a thrust geometry (Lemieux, 1999). The age of these faults were interpreted to be pre-Belly River Group (Campanian) age, constrained by the observation of the reflectors depicting the horizontal undeformed uppermost Upper Cretaceous (Belly River Group and younger) strata overlying F5 in the seismic section.

About 22 km to the west of the F1 fault is a linear offset that was referred to as the West Stand Off Fault (WSOF) (Figure 13) after the community of Stand Off (Schultz et al., 2015), and can be recognized on all the three horizons mapped (Figures 7–9). The WSOF strikes roughly parallel to the F1 fault. Similarly to the F2, F3, and F5 faults, steep basement fabrics appear to align directly with the position of the WSOF (Figure 5a of Lemieux, 1999). Using 3D reflection-seismic survey data, Galloway et al. (2018) confirmed that the WSOF is a fault striking at ~170° and dipping at ~80° (to the west) through an interval of at least 2300 m, although this feature does not create a detectable offset of reflection-seismic horizons and therefore is not apparent in coherence attribute volumes due to limited vertical resolution of the reflection-seismic data. With the methodology used in this report, the vertical displacement on this fault was found to decrease from 55 to 70 m at the depth of the Devonian–Mississippian Exshaw Formation, to 40–45 m at shallower depth of the Cretaceous BFS, top of Milk River Formation, and the lower Bearpaw Formation flooding surface.

Comparison of the point locations of the five faults recognized by Lemieux (1999) with our offset maps indicates that they are closely related to, or overlap with, the five major NW–SE striking linear offsets mapped from the top surface of the Milk River Formation and the BFS (Figures 8, 9, and 13). The linear offsets related to faults F1 and F2 and the northern extension of the linear offset related to fault F3 were also recognized from the much younger lower Bearpaw Formation flooding surface (Figure 7). In areas where Lemieux (1999) mapped the F3, F4, and F5 faults, the lower Bearpaw Formation flooding surface was eroded. The coincidence of the point locations of faults recognized by Lemieux (1999) with the linear offsets mapped in this study allows us to track them in three dimensions (Figures 7–9; Table 1). Offsetting of the lower Bearpaw Formation flooding surface suggests that these faults may have been active after deposition of the lower Bearpaw Formation.

Table 1 summarizes the offsets of these faults. The offsets for the geological units below the BFS were estimated by Lemieux (1999) using an average velocity of 4500 m/s for the sedimentary section for the conversion to depth. Although faults F1 to F5 were recognized in the sedimentary section, steep basement fabrics were recognized to align with F2, F3, and F5 (Lemieux, 1999), suggesting that the positioning of these extensional faults may have been controlled by basement structure.

Table 1. Offsets of faults F1–F5 as shown in Figure 13.

Geological Units	F1 Fault	F2 Fault	F3 Fault	F4 Fault	F5 Fault
Lower Bearpaw Formation	~180 m	~155 m	Eroded	eroded	eroded
Milk River Formation	~190 m	~190 m	~40 m	~60 m	~70 m
BFS	~200 m	~160–200 m	~35 m	~55 m	~90 m
Lower Cretaceous*					~135 m
Jurassic*					~110 m
Mississippian*					~155 m
Cambrian and Devonian*	~235 m	~340 m	~110 m	~155 m	~110 m
Basement*		Steep fabrics	Steep fabrics		

* Note: offsets for the geological units below the base of the Fish Scales Formation (BFS) were estimated by Lemieux (1999)

6 Conclusions

Numerous linear offset structures have been recognized in the southern Alberta Plains 50–140 km east of the Foothills triangle zone. These structures trend southeasterly in the study area north of Lethbridge; they trend south–southeasterly in the area south of Lethbridge. Some of the offset lineaments overlap with faults previously identified at point locations; this confirms the interpretation of those offsets as faults and significantly improves our understanding of the seismically detected faults by adding orientation and extent to these faults. In addition, our offset lineaments map revealed numerous, previously unrecognized structures, and one of the mapped offsets has been confirmed to be a fault with 3D reflection-seismic survey data (Galloway et al., 2018). Interpreted offsets in this study highlight areas of geological interest for future structural analysis.

7 References

Alberta Geological Survey (2019): Alberta Table of Formations; Alberta Energy Regulator, URL <https://ags.aer.ca/publications/Table_of_Formations_2019.html> [November 2019].

Arnott, R.W.C. and Hein, F.J. (1986): Submarine canyon fills of the Hector Formation, Lake Louise, Alberta: Late Precambrian syn-rift deposits of the proto-Pacific miogeocline; Bulletin of Canadian Petroleum Geology, v. 34, p. 395–407.

Baird, A.K., Baird, K.W. and Morton, D.M. (1971): On deciding whether trend surfaces of progressively higher order are meaningful: discussion; GSA Bulletin, v. 82, 1219–1234.

Beaumont, C. (1981): Foreland basins; Geophysical Journal of the Royal Astronomical Society, v. 65, p. 291–329.

Berger, Z. and Zaitlin, B.A. (2011): Detection and analysis of structurally controlled enhanced reservoir potential in mature and emerging oil resource plays in the WCSB: tight oil examples from the Nordegg and Alberta Bakken; Abstract to Recovery – 2011 CSPG CSEG CWLS Convention, p. 1–3.

Berger, Z. and Mushayandevu, M. (2013): Detection and analysis of structurally controlled sweet spots in the Bakken/Three Fork oil shale play of the Williston Basin and the Exshaw/Big Valley oil shale play of the foreland basin of Southern Alberta and Northern Montana; GeoConvention 2013, Integration: Geoscience Engineering Partnership, 6–12 May 2013, Calgary, AB, Canada, p. 1–5.

Davis, J. C. (2002): Statistical and Data Analysis in Geology (3rd edition), John Wiley and Sons, New York, 656 p.

Eaton, D.W., Ross, G.M. and Clowes, R.M. (1999): Seismic-reflection and potential-field studies of the Vulcan structure, western Canada: a Paleoproterozoic Pyrenees? Journal of Geophysical Research, v. 104, p. 255–269.

Evans, K.V., Aleinikoff, J.N., Obradovich, J.O. and Fanning, C.M. (2000): SHRIMP U-Pb geochronology of volcanic rocks, Belt Supergroup, western Montana: Evidence for rapid deposition of sedimentary strata; Canadian Journal of Earth Sciences, v. 37, p. 1287–1300.

Evenchick, C.A., McMechan, M.E., McNicoll, V.J. and Carr, S.D. (2007): A synthesis of the Jurassic–Cretaceous tectonic evolution of the central and southeastern Canadian Cordillera: Exploring links across the orogeny; *in* Whence the Mountains? Inquiries into the Evolution of Orogenic Systems: A Volume in Honor of Raymond A. Price, Sears, J.W., Harms, T.A., and Evenchick, C.A. (ed.),Geological Society of America Special Paper 433, p. 117–145.

Gervais, F., and Brown, R.L. (2011): Testing modes of exhumation in collisional orogens: Synconvergent channel flow in the southeastern Canadian Cordillera, Lithosphere, v. 3(1), p. 55–75.

Gervais, F., Brown, R.L., and Crowley, J.L. (2010): Tectonic implications for a Cordilleran orogenic base in the Frenchman Cap dome, southeastern Canadian Cordillera, Journal of Structural Geology, v. 32, p. 941–959.

Galloway, E., Hauck, T., Corlett, H., Pana, D. and Schultz, R. (2018): Faults and associated karst collapse suggest conduits for fluid flow that influence hydraulic fracturing-induced seismicity; Proceedings of the National Academy of Sciences, v. 115(43), p. E10003–E10012, doi: 10.1073/pnas.1807549115.

Glombick, P., Hathway, B., Mei, S., Banks, C. and Hay, D. (2010): Mapping the Belly River Group in Alberta; General Poster Session, GeoCanada 2010 – Working with the Earth, May 10–14, 2010, Calgary, Canada.

Glombick, P. and Mumpy, A.J. (2014): Subsurface stratigraphic picks for the Milk River 'shoulder,' Alberta Plains: Including tops for the Milk River Formation and Alderson Member of the Lea Park Formation; Alberta Energy Regulator, AER/AGS Open File Report 2013-17, 23 p.

Grant, F.A. (1957): A problem in the analysis of geophysical data; Geophysics, v. 22, p. 309–344.

Hein, F.J. and McMechan, M.E. (1994): Proterozoic and Lower Cambrian strata of the Western Canada Sedimentary Basin; *in* Geological Atlas of the Western Canada Sedimentary Basin, Mossop, G. and Shetsen, I. (comp.), Calgary, Canada, Canadian Society of Petroleum Geologists and Alberta Research Council, p. 57–67.

Hiebert, S.N. and Spratt, D.A. (1996): Geometry of the thrust front near Pincher Creek, Alberta; Bulletin of Canadian Petroleum Geology, v. 44(2), p. 195–201.

Hope, J., Eaton, D.W. and Ross, G.M. (1999): Lithoprobe seismic transect of the Alberta Basin: compilation and overview; Bulletin of Canadian Petroleum Geology, v. 47(4), 331–345.

Höy, T. (1992): Geology of the Purcell Supergroup in the Fernie west-half map area, southeastern British Columbia; British Columbia Ministry of Energy, Mines and Petroleum Resources Bulletin, v. 84, 157 p.

Irish, E.J.W. (1968): Lethbridge, Alberta; Geological Survey of Canada, Map 20-1967 (1:253,440 scale).

Jerzykiewicz, T. (1997): Stratigraphic framework of the uppermost Cretaceous to Paleocene strata of the Alberta Basin; Geological Survey of Canada, Bulletin 510, 121 p.

Kanasewich, E.R., Clowes, R.M. and McCloughan, C.H. (1968): A buried Precambrian rift in western Canada; Tectonophysics, v. 8, p. 513–527.

Lerand, M.M. (1983): Sedimentology of the Blood Reserve sandstone in southern Alberta; Canadian Society of Petroleum Geologists Guidebook, 55 p.

Lemieux, S. (1999): Seismic reflection expression and tectonic significance of Late Cretaceous extensional faulting of the Western Canadian Sedimentary Basin in southern Alberta; Bulletin of Canadian Petroleum Geology. v. 47(4), p. 375–390.

Lemieux, S., Ross, G.M. and Cook, F.A. (2000): Crustal Geometry and tectonic evolution of the Archean crystalline basement beneath the southern Alberta Plains, from new seismic reflection and potential-field studies; Canadian Journal of Earth Sciences. v. 37, p. 1473–1491.

Lukie, T.D., Ardies, G.W., Dalrymple, R.W. and Zaitlin, B.A. (2002): Alluvial architecture of the Horsefly unit (Basal Quartz) in southern Alberta and northern Montana: influence of accommodation changes and contemporaneous faulting; Bulletin of Canadian Petroleum Geology, v. 50, p. 73–91.

Lydon, J.W. (2007): Geology and metallogeny of the Belt-Purcell Basin; *in* Mineral Deposits of Canada: A Synthesis of Major Deposit-Types, District Metallogeny, the Evolution of Geological Provinces, and Exploration Methods, Goodfellow, W.D. (ed.), Geological Association of Canada, Mineral Deposits Division, Special Publication 5, p. 581–607.

Mei, S. (2009): Geologist-controlled trend versus computer-controlled trend: introducing a high-resolution approach to subsurface structural mapping using well-log data, trend surface analysis and geospatial analysis; Canadian Journal of Earth Sciences, v. 46, p. 309–329.

Mei, S., Pana D. and Schultz R. (2015): Mapping formation-top offsets in southwest Alberta, Canada: Methodology and results; extended abstract, GeoConvention 2015 – Geoscience new horizons, May 4–8, 2015, Calgary, Canada, 5 p.

Mei, S. (2020): Formation-top offsets in west-central Alberta and their implications for subsurface structure; Alberta Energy Regulator / Alberta Geological Survey, AER/AGS Open File Report 2020-03, 25 p.

McMechan, M.E. and Thompson, R.I. (1989): Structural style and history of the Rocky Mountain fold and thrust belt; *in* Western Canada Sedimentary Basin: A Case Study, Ricketts, B.R. (ed.), Canadian Society of Petroleum Geologists, Calgary, p. 47–71.

McMechan, M.E. and Thompson, R.I. (1992): The Rocky Mountains; Chapter 17, Part E, *in* Geology of the Cordilleran Orogen in Canada, Gabrielse, H. and Yorath, C.J. (ed.), Geological Survey of Canada, Geology of Canada, no. 4, (also Geological Society of America, The Geology of North America, v. (G-2), p. 635–642.

Monger, J.W.H. (1984): Cordilleran tectonics: A Canadian perspective; Bulletin of the Geological Society of France, v. XXXVI-7, p. 255–278.

Monger, J.W.H. (1989): Overview of Cordilleran geology; Chapter 2; *in* Western Canada Sedimentary Basin: A Case History, Ricketts, B.D. (ed.), Canadian Society of Petroleum Geologists, Calgary, p. 9–32.

Monger, J.W.H. and Price, R.A. (2002): The Canadian Cordillera: Geology and tectonic evolution; Canadian Society of Exploration Geophysicists, Recorder, February 2002, p. 17–36.

Murphy, D.C., van der Heyden, P., Parrish, R.R., Klepacki, D.W., McMillan, W., Struik, L.C., and Gabites, J. (1995): New geochronological constraints on Jurassic deformation of the western edge of North America, southeastern Canadian Cordillera; *in* Jurassic Magmatism and Tectonics of the North American Cordillera, Miller, D.M., and Busby, C. (ed.), Geological Society of America Special Paper 299, p. 159–171.

Pana, D.I. and van der Pluijm, B.A. (2015): Orogenic pulses in the Alberta Rocky Mountains: Radiometric dating of major faults and comparison with the regional tectono-stratigraphic record; Geological Society of America Bulletin, v. 127(3–4), p. 480–502.

Price, R.A. (1973): Large-scale gravitational flow of supracrustal rocks, southern Canadian Rocky Mountains; *in* Gravity and Tectonics, De Jong, K.A., and Scholten, R.A. (ed.), Wiley-Interscience, New York, p. 491–502.

Price, R.A. (1981): The Cordilleran foreland thrust and fold belt in the southern Canadian Rocky Mountains; *in* Thrust and Nappe Tectonics, McClay, K.R., and Price, N.J. (ed.), Geological Society of London, London, p. 427–448.

Prior, G.J., Hathway, B., Glombick, P.M., Pana, D.I., Banks, C.J., Hay, D.C., Schneider, C.L., Grobe, M., Elgr, R. and Weiss, J.A. (2013): Bedrock geology of Alberta; Alberta Energy Regulator, Map 600, URL <https://ags.aer.ca/publications/MAP_600.html#summary> [November 2019].

Ross, G.M. (1991): Tectonic setting of the Windermere Supergroup revisited; Geology, v. 19, p. 1125–1128.

Ross, M.G. and Arnott, R.W. (2006): Regional geology of the Windermere Supergroup, southern Canadian Cordillera and stratigraphic setting of the Castle Creek study area; AAPG Studies in Geology, v. 56, p. 1–16.

Ross, G.M., Mariano, J., Dumont, R., Kjarsgaard, B.A. and Teskey, D. (1997): Was Eocene magmatism widespread in the subsurface of southern Alberta? Evidence from new aeromagnetic anomaly data; *in* Exploring for minerals in Alberta: Geological Survey of Canada, Canada-Alberta agreement on mineral development (1992–1995), R.W. Macqueen (ed.), Geological Survey of Canada Bulletin 500, p. 235–246.

Ross, G.M. and Villeneuve, M. (2003): Provenance of the Mesoproterozoic (1.45 Ga) Belt basin (western North America): Another piece in the pre-Rodinia paleogeographic puzzle; Geological Society of America Bulletin, v. 115(10), p. 1191–1217.

Russell, L.S. and Landes, R.W. (1940): Geology of the southern Alberta Plains; Geological Survey of Canada, Department of Mines and Resources, Mines and Geology Branch, Bureau of Geology and Topography, Memoir 221, p.1– 128.

Schultz, R., Mei, S., Pană, D., Stern, V., Gu, Y.J., Kim, A., & Eaton, D. (2015). The Cardston earthquake swarm and hydraulic fracturing of the Exshaw Formation (Alberta Bakken play); Bulletin of the Seismological Society of America, v. 105(6), p. 2871–2884.

Sears, J.W. (2007): Belt-Purcell Basin: Keystone of the Rocky Mountain fold-and-thrust belt, United States and Canada; *in* Whence the Mountains? Inquiries into the Evolution of Orogenic Systems: A Volume in Honour of Raymond A. Price, Sears, J.W., Harms, T.A. and Evenchick, C.A. (ed), Geological Society of America Special Paper 433, p. 147–166.

Sheriff, R.E. (1991): Encyclopedic dictionary of exploration geophysics; Society of Exploration Geophysicists, Tulsa, 376 p.

Skuce, A.G., Goody, N.P. and Maloney, J. (1992): Passive-roof duplexes under the Rocky Mountain foreland basin, Alberta; American Association of Petroleum Geologists Bulletin, v. 76, p. 67– 80.

Stockmal, G.S., Issler, D.R. and Lebel, D. (1997): Early to middle Eocene thrusting, outer Foothills belt, southern Alberta: Evidence from apatite fission track data; *in* Program with Abstracts, Beauchamp, B. (comp.), CSPG–SEPM 1997 Joint Convention, 1–6 June 1997, Calgary, Alberta, Canada, p. 270.

Struik, L.C. (1988): Crustal evolution of the eastern Canadian Cordillera; Tectonics, v. 7, p. 727–747.

Taylor, J.R. (1997): An introduction to error analysis the study of uncertainties in physical measurements (2nd edition) [electronic resource]; Sausalito, Calif: University Science Books, 1997, xvii, 327 p.

Tinker, S.W. (1996): Building the 3-D jigsaw puzzle: applications of sequence stratigraphy to 3-D reservoir characterization, Permian Basin; American Association of Petroleum Geologists Bulletin, v. 80(4), p. 460–485.

Withjack, M.O., Olson, J. and Peterson, E. (1990): Experimental models of extensional forced folds; American Association of Petroleum Geologists Bulletin, v. 74, p. 1038–1054.

Wren, A.E. (1973): Trend surface analysis – A review; Canadian Journal of Exploration Geophysics, December, p. 39–44.

Wright, G.N., McMechan, M.E. and Potter, D.G. (1994): Chapter 3: Structure and architecture of the Western Canada Sedimentary Basin; *in* Geological Atlas of the Western Canada Sedimentary Basin. G.P. Mossop and I. Shetsen (comp.), Canadian Society of Petroleum Geologists and Alberta Research Council, Alberta Geological Survey, Calgary, p. 25–40.

Zaitlin B. A., Berger Z., Kennedy J. and Kehoe S. (2011): The Alberta Bakken: A potential new, unconventional tight oil resource play; Recovery - 2011 CSPG CSEG CWLS Convention, 9–13 May 2011, Calgary, Canada. p. 1–4.